Large energy-loss straggling of swift heavy ions in ultra-thin active silicon layers*

Zhang Zhan-Gang(张战刚)[a)b)†], Liu Jie(刘 杰)[a)‡], Hou Ming-Dong(侯明东)[a)], Sun You-Mei(孙友梅)[a)], Zhao Fa-Zhan(赵发展)[c)], Liu Gang(刘 刚)[c)], Han Zheng-Sheng(韩郑生)[c)], Geng Chao(耿 超)[a)b)], Liu Jian-De(刘建德)[a)], Xi Kai(习 凯)[a)b)], Duan Jing-Lai(段敬来)[a)], Yao Hui-Jun(姚会军)[a)], Mo Dan(莫 丹)[a)], Luo Jie(罗 捷)[a)b)], Gu Song(古 松)[a)b)], and Liu Tian-Qi(刘天奇)[a)b)]

[a)] *Institute of Modern Physics, Chinese Academy of Sciences, Lanzhou* 730000, *China*
[b)] *University of Chinese Academy of Sciences, Beijing* 100049, *China*
[c)] *Institute of Microelectronics, Chinese Academy of Sciences, Beijing* 100029, *China*

(Received 16 January 2013; revised manuscript received 3 April 2013)

Monte Carlo simulations reveal considerable straggling of energy loss by the same ions with the same energy in fully-depleted silicon-on-insulator (FDSOI) devices with ultra-thin sensitive silicon layers down to 2.5 nm. The absolute straggling of deposited energy decreases with decreasing thickness of the active silicon layer. While the relative straggling increases gradually with decreasing thickness of silicon films and exhibits a sharp rise as the thickness of the silicon film descends below a threshold value of 50 nm, with the dispersion of deposited energy ascending above ±10%. Ion species and energy dependence of the energy-loss straggling are also investigated. For a given beam, the dispersion of deposited energy results in large uncertainty on the actual linear energy transfer (LET) of incident ions, and thus single event effect (SEE) responses, which pose great challenges for traditional error rate prediction methods.

Keywords: single event effects, energy-loss straggling, ultra-thin silicon layer, Monte Carlo simulation

PACS: 61.82.Fk, 02.50.Ng, 61.80.Jh **DOI:** 10.1088/1674-1056/22/9/096103

1. Introduction

As one of the critical reliability issues for modern space-borne integrated circuits (ICs),[1–3] single event effects (SEEs) originate from the particle-induced energy loss in the active silicon layers of electronic devices. However, due to the statistical nature of ion–matter interactions, the energy deposited by the same ions with the same energy in thin silicon layers may exhibit large dispersion, which has been studied for a long time.[4–9] Many approaches have been applied in addressing this issue. In 1988 and 1990, Bichsel[4,5] reviewed the methods for calculating the distribution of deposited energy. Xapsos *et al.* presented an analytical formulation for the fluctuations of deposited energy in 1993[6] and applied the microdosimetry theory to calculate the energy-loss straggling in sensitive volumes (SVs) of microelectronic devices in 2001.[7] Barak and Akkerman[8] calculated the straggling function of the deposited energy in submicron volumes using a dedicated Monte Carlo code and the convolution methods. More recently, Raine *et al.*[10] experimentally quantified the amount of deposited energy dispersion in thin silicon layers down to 100 nm, showing that heavy ion-induced deposited energy dispersion increases with decreasing thickness of sensitive layers, but with a large difference between experimental and simulated results.

With technologies further downscaling, fully-depleted devices such as planar silicon-on-insulator (SOI) or fin-type devices are known as promising device structures for continuing to exploit Moore's law. While the active silicon layers of those advanced structures can be ultra-thin, even on the order of a few nanometers.[11–20] Considering that those ultra-thin silicon films contain only a few tens of silicon atomic layers, i.e., worse statistics than earlier thin films, the energy-loss straggling by the direct ionization process in nano films will be more pronounced and needs detailed analysis. However, few data has been published dealing with the variations of deposited energy in ultra-thin active silicon layers and the potential inadequacies of current error rate prediction methods.

Thus, this paper focuses on an in-depth investigation of energy-loss straggling in device structures with an ultra-thin active silicon layer (such as advanced fully-depleted SOI (FDSOI) devices) by Monte Carlo simulations. The influences of the thickness of silicon films, ion species, and energy on the deposited energy dispersion are also explored to get further insights. Considerable straggling of energy loss results in a great uncertainly of actual linear energy transfer (LET) in ultra-thin active silicon films. Compared to the experimental data of partially-depleted SOI (PDSOI) devices induced by heavy ions, the shape of SEE cross section versus LET curves for FDSOI devices with ultra-thin silicon films is predicted to be significantly changed.

*Project supported by the National Natural Science Foundation of China (Grant Nos. 11179003 and 10975164).
†Corresponding author. E-mail: zhangang@impcas.ac.cn
‡Corresponding author. E-mail: j.liu@impcas.ac.cn

The physics of energy-loss straggling is reviewed in Section 2. Section 3 describes the Monte Carlo simulations in detail. Simulated results and analysis are presented in Section 4, including energy-loss straggling in silicon films with various thicknesses and the impact of ion species and energy. The implications for ground-based testing and error rate prediction are discussed.

2. Physics of energy-loss straggling

When penetrating through a target, swift heavy ions lose energy mainly by stochastic collisions with the target electrons or nuclei. For each ion in a monoenergetic and unidirectional beam, the number of those collision events along the trajectory caused by incident ions is randomized and the energy transferred to a target electron or nucleus in each collision event is also randomized. Thus, the deposited energy E in the target follows the Gaussian distribution[21]

$$\frac{n(E)}{n} = \frac{1}{a\pi^{1/2}} \exp\left[-\frac{(E-E_{\rm av})^2}{a^2}\right], \quad (1)$$

$$a = 2\sqrt{2}Z_1 e^2 \left[\pi Z_2 N t\right]^{1/2}, \quad (2)$$

where $n(E)$ is the number of ions with deposited energy between E and $E + {\rm d}E$, n is the total number of ions, $E_{\rm av}$ is the average deposited energy, a is the straggling parameter which means half width of the energy spectrum at 1/e of the spectrum height, $Z_1 e$ is the charge of the projectile, $Z_2 N$ is the electron density of the target, and t is the thickness of the target.

The full width at half maximum (FWHM) of the energy spectrum is often used to quantify the absolute straggling of energy loss

$$S_{\rm a} = {\rm FWHM} = \frac{2.36}{\sqrt{2}} a = 4.72 Z_1 e^2 \left(\pi Z_2 N t\right)^{1/2}. \quad (3)$$

Assuming that the ion LET keeps constant in the thin silicon layer, i.e., equals the ion LET at the surface of silicon layer, ${\rm LET}_{\rm sur}$. The relative straggling of energy loss is

$$S_{\rm r} = \pm\frac{S_{\rm a}}{2E_{\rm av}} \times 100\% = \pm\frac{2.36 Z_1 e^2 \left(\pi Z_2 N\right)^{1/2}}{{\rm LET}_{\rm sur} t^{1/2}} \times 100\%. \quad (4)$$

In addition, the absolute straggling of energy loss can be transferred to absolute LET straggling if normalized to the thickness of silicon film. The relative straggling of energy loss is equivalent to relative LET straggling.

3. Description of Monte Carlo simulations

The Monte Carlo transport of ions in matter (TRIM) program included in the stopping and range of ions in matter (SRIM-2008.04) software[22,23] was used to investigate the energy-loss straggling of swift heavy ions in device structures with various thicknesses of silicon film for different ion species and energies. The TRIM allows detailed tracking of ion trajectories in the target and recording the ion energies, momenta, positions, and angles of transmitted ions. The calculation type "ion distribution and quick calculation of damage" in TRIM was used to obtain the energy loss by direct ionization and the coulomb scattering for each ion, but without further calculating cascades and hence limiting the calculation to the ion trajectories, since the primary focus of this work is the deposited energy straggling in direct ionization process.

The device model used in the simulations is shown in Fig. 1. The ultra-thin silicon layer is sandwiched by the top overlayers and bottom buried oxide (BOX). The top overlayers which comprise passivation layer, metallization layers, plugs, etc. are represented by a 5-μm-thick SiO_2 layer for convenient comparison between the straggling of deposited energy in different technology generations. In each simulation run, the monoenergetic and point-like incoming beams with 10^5 ions were used to strike the device model. All the ions were at normal incidence. Thanks to the SRIM supporting software modules (S^3M),[24] the deposited energy in the ultra-thin silicon layer can be conveniently extracted and analyzed in a histogram.

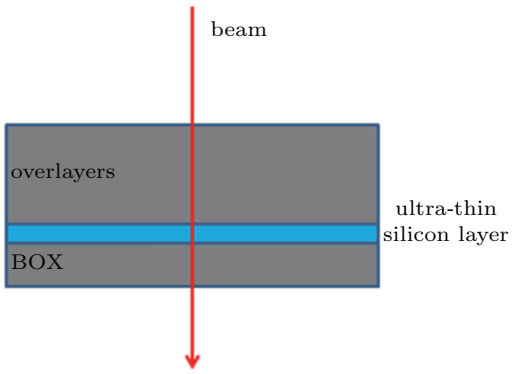

Fig. 1. (color online) Device model used in Monte Carlo simulations (not scale). The deposited energy was recorded in the ultra-thin silicon layer, located after 5-μm-thick SiO_2 overlayers.

4. Simulation results and analysis

The simulation results are presented below in the following order. First, the energy-loss straggling in silicon films of various thicknesses is reported and analyzed, showing consistent results with theoretical calculations in Section 2. Then, the ion species and energy dependence of energy-loss straggling in ultra-thin silicon films are investigated.

4.1. Energy-loss straggling in silicon films with various thicknesses

In the beginning, the energy-loss spectrum of 500-MeV ^{86}Kr ions in 5-nm-thick silicon film (representative of IBM's 22-nm extremely thin SOI complementary metal-oxide-semiconductor (CMOS) technology[11]) is reported in Fig. 2.

For the given beam with LET_{sur} of 38.03 MeV/(mg/cm^2), the deposited energy in device's active silicon layer exhibits wide spread, ranging from 10.5 keV to 84.4 keV with an average deposited energy of 45.4 keV. The absolute straggling (i.e., FWHM) and relative straggling of energy loss (see Eq. (4)) are 26.2 keV and ±28.8%, respectively. The high variations in the energy deposited by the same ion with the same energy will cause large uncertainty on actual LET, and hence device responses. It should be mentioned that several events with abnormally high deposited energy are not shown in Fig. 2 and will be discussed in the next section.

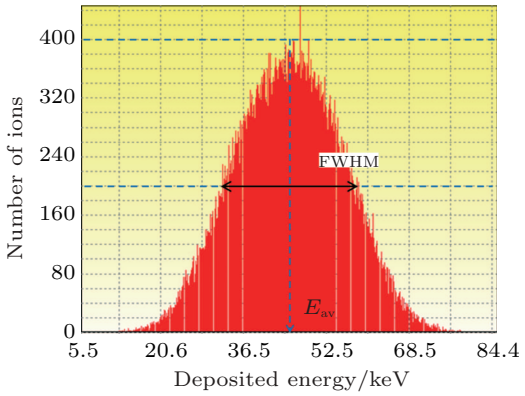

Fig. 2. (color online) Number of ions as a function of energy loss by 500 MeV ^{86}Kr ions in 5-nm-thick silicon film. The FWHM and E_{av} of the spectrum are measured for calculating the relative straggling of energy loss.

Table 1. Energy-loss straggling in silicon films with various thicknesses for ^{86}Kr ion species. The initial energy equals 500 MeV, and LET_{sur} equals 38.03 MeV/(mg/cm^2).

T_{si}/nm	E_{av}/keV	FWHM/keV	±FWHM/2E_{av}×100%
2.5	23.3	16.7	±35.9%
5	45.4	26.2	±28.8%
7.5	67.6	31.7	±23.5%
10	89.6	37.6	±21%
20	178.1	56.5	±15.9%
40	355	84.5	±11.9%
50	443.7	91.1	±10.3%
75	664.8	114.1	±8.6%
100	885.9	123.6	±7%
150	1328.4	149	±5.6%
200	1770.5	190.1	±5.4%
250	2213.5	206.7	±4.7%
300	2656.2	247.4	±4.7%
500	4427.9	325.8	±3.7%
1000	8865.2	417.9	±2.4%

The trend of energy-loss straggling for different thicknesses of silicon film, T_{si}, from 1000 nm down to 2.5 nm, is further investigated. For convenience of comparison, the absolute straggling and relative straggling of energy loss for each device structure were extracted or calculated from the original energy-loss spectra (see Table 1) and plotted as functions of T_{si} in Fig. 3. Not as one might expect (worse statistics in thinner silicon film and thus larger energy-loss straggling), the absolute straggling of energy loss shows continuous roll-off with decreasing thickness of silicon film. Whereas the relative straggling of energy loss increases gradually with thinner silicon film and a sharp increase happens as the film's thickness descends below a threshold of 50 nm, with deposited energy dispersion ascending above ±10%. In addition, the thickness as low as 2.5 nm (representative of 18-nm strained FDSOI CMOS technology[12]) was simulated, showing that the corresponding energy-loss straggling is up to ± 35.9%.

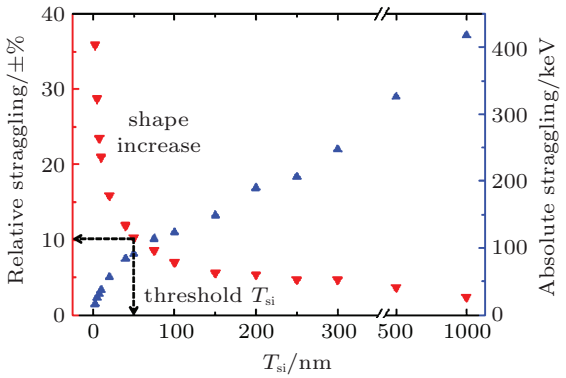

Fig. 3. (color online) Absolute straggling (blue up-triangle symbols) and relative straggling (red down-triangle symbols) of deposited energy as a function of silicon film thickness (500 MeV ^{86}Kr ions).

4.2. Different ion species with the same energy

The ion species dependence of energy-loss straggling is explored, with fixed ion energy per nucleon. Based on Eq. (4), the charge of incident ions, Z_1e, is directly related to the energy-loss straggling. The charge of a projectile in thin target (μg/cm^2) can be expressed by the equilibrium charge which depends on the projectile's velocity and atomic number z_1.[25] However, charged particles are considered to lose all the electrons in the front layers (e.g., detector, degraders, metallization layers, etc.) before reaching the active silicon layer, if the projectile's velocity is above the threshold velocity needed for projectile acquiring target electrons, $qv_0/z_1^{1/3}$, where q is the initial charge of the projectile, and v_0 is the Bohr velocity (25 keV/u).[26] Consequently, the charge of incident ions, Z_1e, can be replaced by z_1e in Eqs. (3) and (4) for most cases of accelerator testing.

Simulations were performed for five kinds of beams (see Table 2) with the same energy per nucleon (10 MeV/n) striking the device structure with a 5-nm-thick active silicon layer. As shown in Fig. 4, the absolute straggling of energy loss increases linearly with heavier ion species, whereas the relative straggling descends at first and tends to be constant with increasing atomic number of projectiles.

Table 2. Energy-loss straggling for different ion species, with the same energy per nucleon. The initial energy is 10 MeV/n.

Ion species	LET_{sur}/ MeV·cm^2·mg^{-1}	E_{av}/keV	FWHM/keV	$\pm$FWHM/2E_{av} $\times$100%
$^{12}_{6}$C	1.27	1.52	2.21	$\pm$72.7%
$^{40}_{18}$Ar	9.91	11.81	10.95	$\pm$46.4%
$^{86}_{36}$Kr	31.85	38.05	26.32	$\pm$34.6%
$^{132}_{54}$Xe	59.74	71.43	40.37	$\pm$28.3%
$^{209}_{83}$Bi	91.24	108.96	63.04	$\pm$28.9%

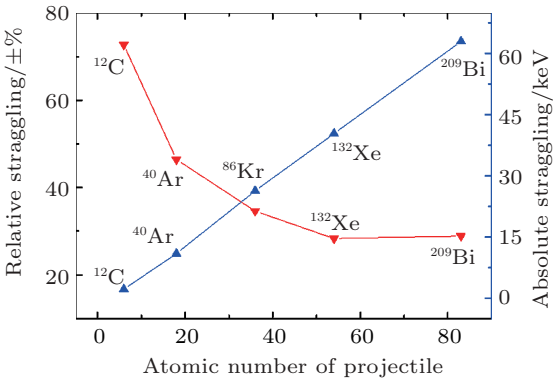

Fig. 4. (color online) The absolute straggling (blue up-triangle symbols) and relative straggling (red down-triangle symbols) of deposited energy in 5-nm-thick silicon film as a function of the atomic number of the projectile, with the same energy per nucleon of 10 MeV/n.

4.3. Different ion energies for the same ion

The impact of ion energy on energy-loss straggling is also studied, with fixed ion species. As shown in Table 3 and Fig. 5, the absolute straggling of energy loss varies little with increasing ion energy (note the scale of the right Y axis). The increase of relative straggling with ion energy results from the decrease of ion LET_{sur}, i.e., decrease of average deposited energy for ions with higher energy. The Bragg peak for the maximum LET is located at $E = 2.33$ MeV/n for ^{86}Kr ions in silicon.

Table 3. Energy-loss straggling for ^{86}Kr ions with different energies per nucleon.

Initial energy/ MeV·n^{-1}	LET_{sur}/ MeV·cm^2·mg^{-1}	E_{av}/keV	FWHM/keV	$\pm$FWHM/2E_{av} $\times$100%
3	40.85	48.67	25.75	$\pm$26.5%
5.8	38.03	45.47	26.18	$\pm$28.8%
10	31.85	38.05	26.32	$\pm$34.6%
15	26	31.05	24.85	$\pm$40%
20	21.81	25.94	23.5	$\pm$45.3%
25	18.9	22.54	22.41	$\pm$49.7%

The results indicate that both ion species and average energy loss are key parameters in determining the relative straggling of energy loss in a given device structure. In order to minimize the energy-loss straggling at a fixed LET value (i.e., fixed average energy loss), lighter ions should be superior to heavier ions during accelerator testing of SEE cross section versus LET (σ-LET) curves for modern ICs.

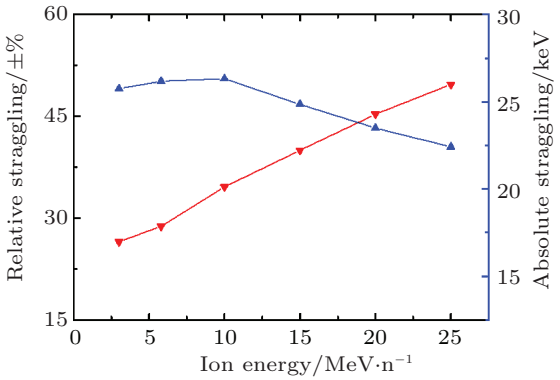

Fig. 5. (color online) The absolute straggling (blue up-triangle symbols) and relative straggling (red down-triangle symbols) of deposited energy in 5-nm-thick silicon film as a function of ion energy for the same ions.

5. Discussion

The ion energy dispersion after penetrating the top overlayers is investigated primarily to make sure that the large energy-loss straggling arises from the ultra-thin silicon film structure. Moreover, the influence of the large dispersion of deposited energy on the device response is then discussed, taking into account the profile of ion track and the size of sensitive volumes. Finally, implications for ground-based testing and error rate prediction are discussed.

5.1. Energy dispersion after penetrating the overlayers

The contribution of top overlayers to energy-loss straggling in the ultra-thin silicon films is discussed. The output energies and positions of 10^5 500-MeV ^{86}Kr ions at the overlayers/silicon interface were recorded by TRIM software and displayed in Figs. 6 and 7, respectively. Note the log scale of the ion number. The energy dispersion after the overlayers are quite small, with absolute and relative energy straggling of about 1 MeV and $\pm$0.1%, respectively, which results from the relatively thick overlayers, i.e., good statistics. The energy dispersion leads to an ion LET_{sur} dispersion of $\pm$0.03%, which can be neglected in comparison to the large LET dispersion in the ultra-thin silicon films.

However, several events with abnormally low output energies should be noted in the asymmetrical energy spectrum, with the probability of $\sim 10^{-4}$. Those events were also observed during the process of energy deposition in the ultra-thin silicon films. The ion paths of those events are tracked and turn out to correspond to the outer ion positions in Fig. 7. Thus, the rare large energy-loss events are attributed to the interactions between the incident ions and target nuclei, creating Si or O recoils. Although with low probability, the impact of those events on the response of device can be of great importance. First, after penetrating through the overlayers, the initial mo-

noenergetic and unidirectional beam exhibits complex characteristics (e.g., energy straggling, output directions, etc.), with the probability of large decrement of ion energy, causing large increment of ion LET_{sur}. Second, energetic recoil nucleus created inside or in the vicinity of sensitive volumes may also affect the device sensitivity.[27]

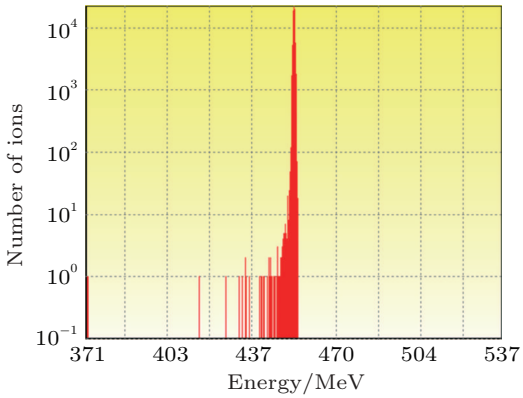

Fig. 6. (color online) Number of ions as a function of ion output energy after the overlayers.

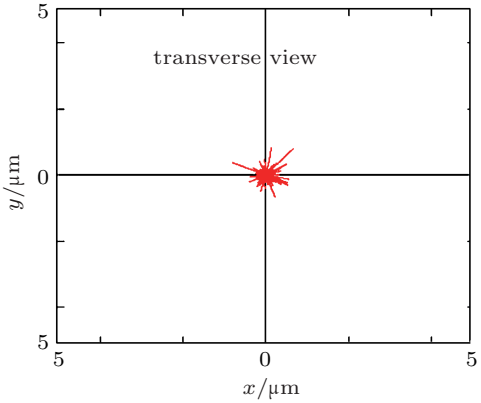

Fig. 7. (color online) View of the cross section at overlayers/silicon interface, showing the particle positions. All the particles strike at the center of the device plane initially.

5.2. Influence of large energy-loss straggling on the device response

In the previous part, the straggling nature of heavy ions-induced energy loss in ultra-thin active silicon layers was discussed, but without considering the profile of ion track and also lateral dimensions of the sensitive volume. In this part, Geant4 v9.4 simulation toolkit[28–30] is applied to model the radial ionization profile of deposited energy induced by heavy ions. As shown in Fig. 8(a), the charge density induced by 500-MeV ^{86}Kr ions in the 5-nm active silicon layer exhibits wide radial distribution. The accumulated generated charge reaches 100% of the total value (about 1.95 fC) at a radial distance of 0.6 μm. This means that only part of the charge in the wide cylinder-shaped ion track can be collected by the narrow sensitive volumes of advanced FDSOI devices (with lateral dimensions on the order of tens of nanometers), which are isolated by the surrounding shallow trench isolation (STI) and BOX materials. This adds uncertainty to the final collected charge at sensitive nodes of nanometric devices, due to the non-uniform distribution of charge density in the heavy ion track. Plus the large uncertainty of the total track charge generated by the same ions with the same energy (due to the large straggling of energy-loss), accurate predictions of SEE response can be a tricky problem for small-geometry devices with ultra-thin sensitive volumes.

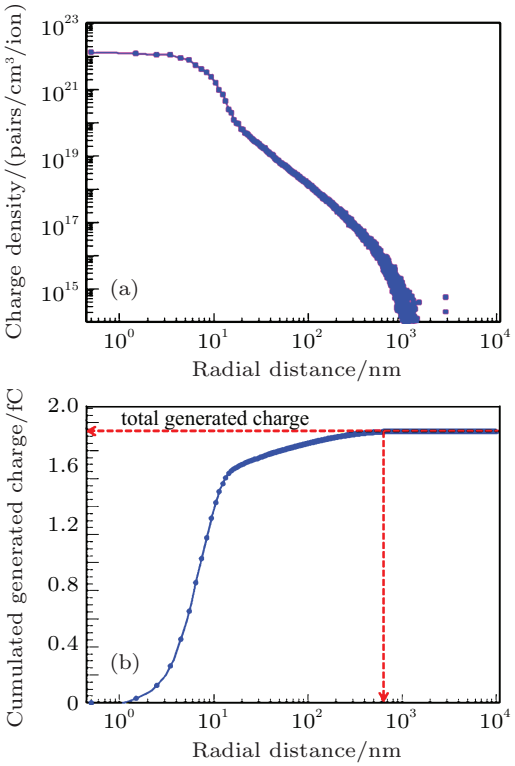

Fig. 8. (color online) Geant4 simulation of (a) the radial pair density profile and (b) the accumulated generated charge as a function of radial distance from the track core for 500-MeV ^{86}Kr ions in 5-nm silicon film, after penetrating 5-μm silica overlayers.

5.3. Implications for ground-based testing and error rate prediction

For many years, LET has been used as an engineering metric in error rate prediction of ICs for space missions. The SEE sensitivity of electronic components in a given radiation environment can be estimated, via getting the plot of SEE cross section versus effective LET in earth-based testing.[31,32] Unfortunately, the large LET dispersion for the same ions with the same energy in ultra-thin silicon layer structures brings great challenges for traditional error rate prediction methods.

Figure 9 shows the single event upset (SEU) cross section of 0.5-μm PDSOI static random access memories (SRAMs) with active silicon layer thickness of about 300 nm, as a function of ion LET. Heavy ion irradiations were performed at the heavy ion research facility in Lanzhou (HIRFL) cyclotrons. Due to the relatively lower LET dispersion in 300-nm-thick silicon film (see Fig. 3), the heavy ion SEU data fit well with

the Weibull curve function. However, as the active silicon layer becomes thinner and thinner, i.e., larger LET dispersion, the shape of traditional σ-LET curve is predicted to be changed in the vicinity of threshold LET, as shown below.

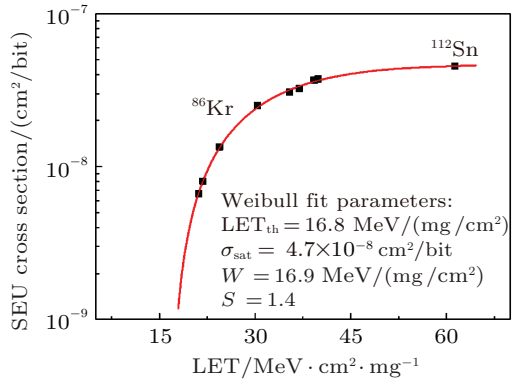

Fig. 9. (color online) Heavy ion experimental data of 0.5-μm PDSOI SRAMs with active silicon layer thickness of about 300 nm. ^{86}Kr and ^{112}Sn beams with initial energy of 25 MeV and 3.7 MeV were used for irradiations at normal incidence, with both ion ranges above 30 μm. The Weibull fit parameters are displayed in the plot. Error bars are smaller than the symbols.

As illustrated in Fig. 10, other than traditional σ-LET curve with sharp decrease near the threshold LET, a long "tail" of the SEE cross section in the sub-$\mathrm{LET_{th}}$ region appears, due to the probability of high energy depositions for ions with LET lower than $\mathrm{LET_{th}}$. The long "tail" results in a $\mathrm{LET_{th}}$ shift to lower LET region. The amount of $\mathrm{LET_{th}}$ shift can be calculated as follows.

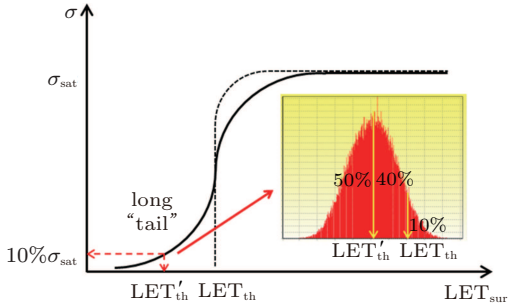

Fig. 10. (color online) Schematic diagram of the shape evolution of σ-LET curve near the threshold LET region, resulting from the large LET dispersion for a given beam in ultra-thin active silicon layers. Dashed line represents the traditional σ-LET curve (without considering the ion LET dispersion), which is displayed in a more ideal way in order to emphasize the impact of ion LET dispersion. $\mathrm{LET_{th}}$ and σ_{sat} represents the threshold LET and saturated cross section of traditional σ-LET curve, respectively. $\mathrm{LET_{th}}\prime$ means the threshold LET of "new" σ-LET curve (solid line, taking the large LET dispersion into consideration), where $\sigma = 10\%\sigma_{\mathrm{sat}}$. The inset shows the Gaussian distribution of ion actual LET in ultra-thin active silicon layers.

As mentioned in the previous section, the energy-loss spectrum of a given beam in ultra-thin silicon films can be converted to the actual LET spectrum of an incident ion if normalized to the thickness of silicon film. The average value of the ion actual LET spectrum is equal to the ion LET at the silicon layer surface, $\mathrm{LET_{sur}}$. The inset of Fig. 10 shows the Gaussian distribution of ion actual LET, with $\mathrm{LET_{sur}}$ smaller than $\mathrm{LET_{th}}$. As 10% of the total incident ions (integral of the spectrum) have actual LET higher than $\mathrm{LET_{th}}$, the average LET of the spectrum will be equal to $\mathrm{LET_{th}}\prime$. Based on the cumulative distribution function (CDF) of Gaussian distribution (see Eq. (1)), the $\mathrm{LET_{th}}$ shift can be written as

$$\mathrm{LET_{th}} - \mathrm{LET'_{th}} = 1.28\frac{\sqrt{2}a}{t}. \tag{5}$$

From Eq. (4), the relative straggling of energy loss (also ion LET) has the form of

$$|S_{\mathrm{r}}| = \frac{0.84}{\mathrm{LET'_{th}}}\frac{a}{t}. \tag{6}$$

The final expression is obtained by combining the above two formulas

$$\mathrm{LET'_{th}} = \frac{1}{1+2.16\,|S_{\mathrm{r}}|}\mathrm{LET_{th}}. \tag{7}$$

It is clearly shown that the amount of $\mathrm{LET_{th}}$ shift depends on the value of the relative straggling of energy loss, which is determined by the silicon film thickness, ion species, and average energy loss. For example for relative straggling of ±28.8% in a 5-nm-thick active silicon layer (500 MeV ^{86}Kr ions), the threshold LET is decreased by a factor of about 40%.

In the practical space radiation environment, the particle flux increases dramatically at lower LET values, as shown in Fig. 11. Note the log scale of integral particle flux. Thus, the considerable threshold LET shift to lower LET value will worsen the on-orbit error rates of advanced devices with ultra-thin active layers.

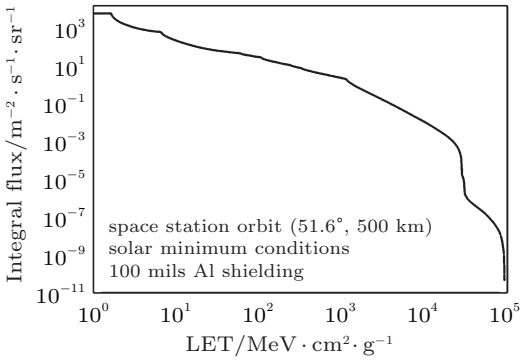

Fig. 11. Particle integral flux as a function of LET at space station orbit (calculated by CREME96[33]).

Another issue relates to the applicability of LET as an engineering metric of SEE testing, which has been questioned in terms of ion species and energy effects for many years.[34] Ions with the same LET, but different ion species and energy, may induce different SEE responses due to nuclear reactions, track structure differences, and so on. Besides that, the ion species dependence of ion LET dispersion (see Fig. 4) further suggests that primary ion LET is not sufficient to describe the beam characteristics, and thus the SEE response of modern devices with ultra-thin active silicon layers.

6. Conclusions

With further downscaling of CMOS technologies, the active silicon layers of advanced FDSOI devices can be extremely thin, even in the order of a few nanometers. The straggling of energy loss by the same ions with the same energy in those ultra-thin active silicon layer structures is investigated by Monte Carlo simulations. For a given ion beam, the actual deposited energy exhibits a wide spread, with relative energy-loss straggling up to $\pm 28.8\%$ in 5-nm active silicon film (500 MeV ^{86}Kr ions). The straggling of deposited energy depends on the thickness of silicon film, ion species, and energy. As silicon film becomes thinner, the absolute straggling of energy loss shows a continuous roll-off, while the relative straggling increases slowly at first and shows a sharp rise as the film thickness descends below a threshold of 50 nm, with deposited energy dispersion ascending above $\pm 10\%$.

The considerable straggling of energy loss in ultra-thin silicon layer structures brings great challenges for traditional error rate prediction method, due to the resulting uncertainty on ion actual LET and hence device responses. Heavy ion experimental data show that the σ-LET curve of PDSOI devices with the thickness of silicon film (about 300 nm) fits well with Weibull curve function. However, the shape of the traditional σ-LET curve near the threshold LET region will be changed in FDSOI devices with ultra-thin silicon films. The emerging long "tail" of SEE cross section at the sub-LET_{th} region leads to a considerable threshold LET shift to a lower LET region which will exacerbate the on-orbit error rate performance of advanced devices with ultra-thin active silicon layers.

Acknowledgement

Heavy ion experiments in this work were conducted at the Heavy Ion Research Facility in Lanzhou (HIRFL), Institute of Modern Physics, Chinese Academy of Sciences (IMPCAS). The authors are grateful for the support of the HIRFL team.

References

[1] Liu Z, Chen S M, Chen J J, Qin J R and Liu R R 2012 *Chin. Phys. B* **21** 099401
[2] Zhang Q X, Hou M D, Liu J, Wang Z G, Jin Y F, Zhu Z Y and Sun Y M 2004 *Acta Phys. Sin.* **53** 566 (in Chinese)
[3] Chen J J, Chen S M, Liang B and Deng K F 2012 *Chin. Phys. B* **21** 016103
[4] Bichsel H 1988 *Rev. Mod. Phys.* **60** 663
[5] Bichsel H 1990 *Nucl. Instrum. Meth. Phys. Res. B* **52** 136
[6] Xapsos M A, Weatherford T R and Shapiro P 1993 *IEEE Trans. Nucl. Sci.* **40** 1812
[7] Xapsos M A, Summers G P, Burke E A and Poivey C 2001 *Nucl. Instrum. Meth. Phys. Res. B* **184** 113
[8] Barak J and Akkerman A 2005 *IEEE Trans. Nucl. Sci.* **52** 2175
[9] Weller R A, Sternberg A L, Massengill L W, Schrimpf R D and Fleetwood D M 2003 *IEEE Trans. Nucl. Sci.* **50** 2265
[10] Raine M, Gaillardin M, Paillet P, Duhamel O, Girard S and Bournel A 2011 *IEEE Trans. Nucl. Sci.* **58** 2664
[11] Cheng K, Khakifirooz A, Kulkarni P, *et al.* 2011 *Symposium on VLSI Technology,* June 14-16, 2011 Kyoto, Japan, p.128
[12] Barral V, Poiroux T, Andrieu F, Buj-Dufournet C, Faynot O, Ernst T, Brevard L, Fenouillet-Beranger C, Lafond D, Hartmann J M, Vidal V, Allain F, Daval N, Cayrefourcq I, Tosti L, Munteanu D, Autran J L and Deleonibus S 2007 *IEEE International Electron Devices Meeting,* December 10-12, 2007 Washington, DC, USA, p. 61
[13] Majumdar A, Wang X L, Kumar A, Holt J R, Dobuzinsky D, Venigalla R, Ouyang C, Koester S J and Haensch W 2009 *IEEE Electron Dev. Lett.* **30** 413
[14] Monfra S, Fenouillet-Beranger C, Bidal G, Boeuf F, Denorme S, Huguenin J L, Samson M P, Loubet N, Hartmann J M, Campidelli Y, Destefanis V, Arvet C, Benotmane K, Clement L, Faynot O and Skotnicki T 2010 *Solid-State Electron.* **54** 90
[15] Fenouillet-Beranger C, Denorme S, Perreau P, *et al.* 2009 *Solid-State Electron.* **53** 730
[16] Majumdar A, Ren Z B, Koester S J and Haensch W 2009 *IEEE Trans. Electron Dev.* **56** 2270
[17] Shin C, Cho M H, Tsukamoto Y, Nguyen B Y, Mazure C, Nikolic B and Liu T J K 2010 *IEEE Trans. Electron Dev.* **57** 1301
[18] Morvan S, Andrieu F, Casse M, *et al.* 2012 *Symposium on VLSI Technology,* June 12-14, 2012 Honolulu, Hawaii, USA, p. 111
[19] Andrieu F, Faynot O, Rochette F, *et al.* 2007 *Symposium on VLSI Technology*, June 12-14, 2007 Kyoto, Japan, p. 50
[20] Majumdar A, Ren Z B, Sleight J W, Dobuzinsky D, Holt J R, Venigalla R, Koester S J and Haensch W 2008 *IEEE Electron Dev. Lett.* **29** 515
[21] Fudan University, Tsinghua University and Peking University 1985 *Nuclear Physics Experimental Methods* (Part I) (2nd edn.) (Beijing: Atomic Energy Press) p. 58 (in Chinese)
[22] Ziegler J F, Biersack J P and Littmark U 1985 *The Stopping and Range of Ions in Solids* (New York: Pergamon Press)
[23] http://www.srim.org/
[24] Pavlovic M and Strasik I 2007 *Nucl. Instrum. Meth. Phys. Res. B* **257** 601
[25] Javanainen A, Trzaska W H, Harboe-Sorensen R, Virtanen A, Berger G and Hajdas W 2010 *IEEE Trans. Nucl. Sci.* **57** 1946
[26] Fudan University, Tsinghua University and Peking University 1985 *Nuclear Physics Experimental Methods* (Part I) (2nd edn.) (Beijing: Atomic Energy Press) p. 49 (in Chinese)
[27] Liu M S, Liu H Y, Brewster N, Nelson D, Golke K W, Kirchner G, Hughes H L, Campbell A and Ziegler J F 2006 *IEEE Trans. Nucl. Sci.* **53** 3487
[28] Agostinelli S, Allison J, Amako K,*et al.* 2003 *Nucl. Instrum. Meth. Phys. Res. A* **506** 250
[29] Allison J, Amako K, Apostolakis J, *et al.* 2006 *IEEE Trans. Nucl. Sci.* **53** 270
[30] http://geant4.cern.ch/
[31] 1996 *EIA/JESD57: Test Procedure for the Measurement of Single-event Effects in Semiconductor Devices from Heavy Ion Irradiation*
[32] 2002 *ESA/SCC Basic Specification No. 25100: Single Event Effects Test Method and Guidelines*
[33] https://creme.isde.vanderbilt.edu/
[34] Reed R A, Weller R A, Mendenhall M H, Lauenstein J M, Warren K M, Pellish J A, Schrimpf R D, Sierawski B D, Massengill L W, Dodd P E, Shaneyfelt M R, Felix J A, Schwank J R, Haddad N F, Lawrence R K, Bowman J H and Conde R 2007 *IEEE Trans. Nucl. Sci.* **54** 2312